### **OPTICS**

## Multioctave supercontinuum generation and frequency conversion based on rotational nonlinearity

John E. Beetar<sup>1</sup>\*, M. Nrisimhamurty<sup>1</sup>\*, Tran-Chau Truong<sup>1</sup>, Garima C. Nagar<sup>2</sup>, Yangyang Liu<sup>1</sup>, Jonathan Nesper<sup>1</sup>, Omar Suarez<sup>1</sup>, Federico Rivas<sup>1</sup>, Yi Wu<sup>1,3,4</sup>, Bonggu Shim<sup>2</sup>, Michael Chini<sup>1,4†</sup>

The field of attosecond science was first enabled by nonlinear compression of intense laser pulses to a duration below two optical cycles. Twenty years later, creating such short pulses still requires state-of-the-art few-cycle laser amplifiers to most efficiently exploit "instantaneous" optical nonlinearities in noble gases for spectral broadening and parametric frequency conversion. Here, we show that nonlinear compression can be much more efficient when driven in molecular gases by pulses substantially longer than a few cycles because of enhanced optical nonlinearity associated with rotational alignment. We use 80-cycle pulses from an industrial-grade laser amplifier to simultaneously drive molecular alignment and supercontinuum generation in a gas-filled capillary, producing more than two octaves of coherent bandwidth and achieving >45-fold compression to a duration of 1.6 cycles. As the enhanced nonlinearity is linked to rotational motion, the dynamics can be exploited for long-wavelength frequency conversion and compressing picosecond lasers.

Copyright © 2020 The Authors, some rights reserved; exclusive licensee American Association for the Advancement of Science. No claim to original U.S. Government Works Distributed under a Creative Commons Attribution NonCommercial License 4.0 (CC BY-NC).

### INTRODUCTION

The temporal confinement of light to durations close to the optical period (1) and the conversion of such few-cycle pulses to extreme ultraviolet (XUV) and x-ray wavelengths (2, 3) have enabled measurement and control of electron dynamics on the sub-femtosecond time scale (4, 5). A prerequisite for entry into the single-cycle regime is the coherent generation of octave-spanning spectra, which can be achieved through nonlinear propagation of multicycle laser pulses through solid, liquid, or gaseous media. The broadened supercontinuum is a hallmark of self-phase modulation (SPM) (6), a nonlinear process governed by the intensity dependent refractive index  $\Delta n_i = n_2 I$  associated with the optical Kerr effect.

Key properties of the Kerr nonlinearity have led to the widespread adoption of laser pulse compression schemes based on SPM in gasfilled capillary fibers (7-10). As the refractive index changes arise because of field-driven distortions of the valence electronic wave function (11), having a natural time scale below 1 fs, the response is effectively instantaneous and the refractive index tracks the timedependent laser intensity I(t). This in turn imparts a nearly linear spectral chirp onto the pulses during propagation, allowing for compression to nearly bandwidth-limited durations with the use of prism pairs, gratings, or chirped mirrors. Furthermore, the tight binding of valence electrons in inert gases allows the use of relatively high laser intensities before the detrimental onset of ionizationrelated dispersion and losses.

Generation of the shortest pulses, and broadest supercontinuum spectra, has therefore been traditionally accomplished by driving the SPM process in noble gas-filled capillary fibers using shorter input pulses (12). Shorter driving pulses allow exposure of the neutral gas atoms to higher laser intensities, or, alternatively, the use of heavier gases with larger  $n_2$ , both resulting in larger nonlinear phase shifts

†Corresponding author. Email: michael.chini@ucf.edu

 $\Delta \phi_{nl}(t) \propto n_2 I(t)$ . To this end, substantial effort has been invested into the development of few-cycle laser amplifiers (13, 14) and two-stage compression schemes (15-17), which mitigate the effects of ionization and plasma generation on the efficiency and compressibility of broad supercontinuum spectra.

Recently, molecular gases (18) have been proposed as an alternative to noble gases for hollow-core fiber (HCF) pulse compressors. For molecular gases, the vibrational and rotational degrees of freedom result in the addition of "delayed" nonlinear responses  $\Delta n_d$  caused by the field-induced alignment and stretching of the molecular bonds (19, 20), as well as four-wave mixing processes associated with Raman transitions (21, 22). In the case of linear molecules, the rotational nonlinearity dominates over the vibrational contribution (23) and has only a minimal impact on the propagation of short pulses (below ~100 fs) because of a lack of temporal overlap with the delayed response (24). However, it has been exploited to imprint temporal phase shifts onto a second copropagating pulse, which arrives during a revival of rotational coherence (25, 26). Conversely, long input pulses (hundreds of femtoseconds) experience a prolonged interaction that can coincide with the delayed response duration (27), markedly increasing the magnitude of the induced rotational nonlinearity, as illustrated in Fig. 1. For sufficiently long pulses, the enhanced rotational nonlinearity can also be considered to be nearly instantaneous and can yield a qualitatively similar time-dependent nonlinear response as that of the electronic Kerr nonlinearity. By appropriately choosing the molecular gas according to the input pulse duration, the total nonlinearity can be enhanced more than 10-fold in comparison to an atomic gas with similar nonlinear susceptibility and ionization potential (27).

Here, we suggest a conceptually new approach to few-cycle pulse compression, wherein the input pulse duration is chosen to optimize the delayed contributions to the nonlinearity rather than minimize the ionization. By taking advantage of the much larger rotational contribution to the nonlinear index of refraction of molecules (27) and using relatively long laser pulses for which the rotational nonlinearity can be nearly instantaneous, we achieve a record >45× pulse compression in a single stage. We also demonstrate the utility of these pulses for applications in attosecond science by generating a

<sup>&</sup>lt;sup>1</sup>Department of Physics, University of Central Florida, Orlando FL 32816, USA. <sup>2</sup>Department of Physics, Applied Physics and Astronomy, Binghamton University, Binghamton NY 13902, USA. <sup>3</sup>Institute for the Frontier of Attosecond Science and Technology, University of Central Florida, Orlando FL 32816, USA. 4CREOL, the College of Optics and Photonics, University of Central Florida, Orlando FL 32816, USA. \*These authors contributed equally to this work.

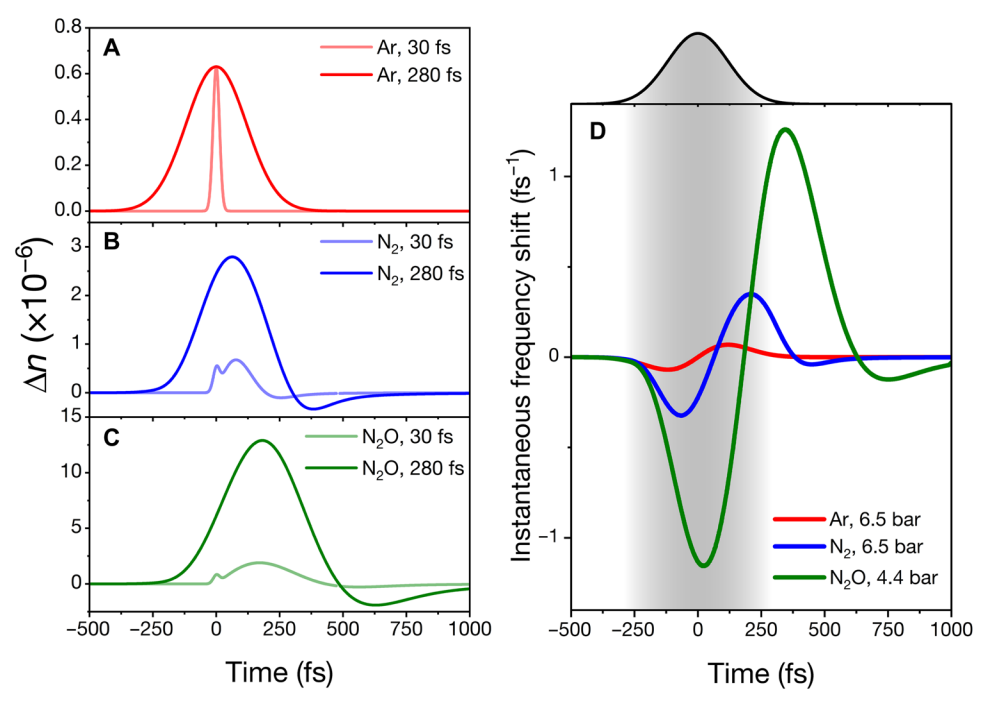


Fig. 1. Nonlinear indices and phase shifts. The nonlinear indices of refraction of Ar,  $N_2$ , and  $N_2$ O (A to C) are calculated for short (30 fs) and long (280 fs) input pulse durations. Ar and  $N_2$  share similar ionization potentials and instantaneous nonlinear refractive indices. Both atomic and molecular systems exhibit an instantaneous response  $\Delta n_i$  due to the electronic Kerr nonlinearity, while the delayed rotational response  $\Delta n_d$ , proportional to the degree of alignment in the molecular ensemble, is present only in the molecular systems. For short input pulses, the effective change in refractive index is approximately the same in Ar and  $N_2$  because only the instantaneous contribution takes effect during the period of interaction, whereas the long pulses see a significantly larger  $\Delta n$  in  $N_2$ . The effect is even more pronounced in  $N_2$ O, which was chosen because of its larger polarizability anisotropy and longer rotational period. The latter plays a crucial role because the degree to which the temporal evolution of the refractive index coincides with the intensity envelope (shown in gray for the 280-fs pulse) determines the shape of temporal phase shift and thus the time dependence of the instantaneous frequency (D).

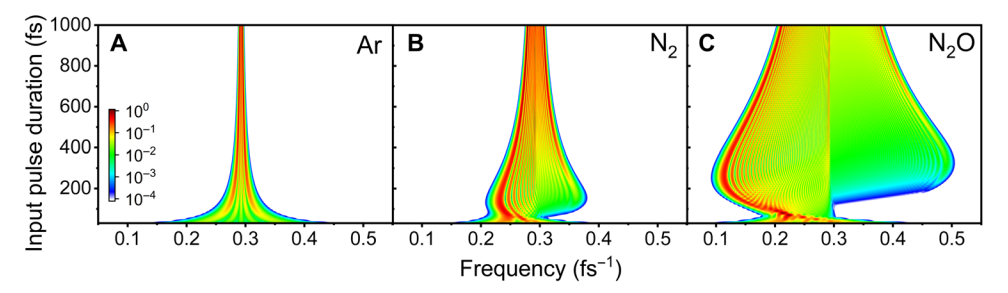


Fig. 2. Pulse duration dependence of spectral broadening. Comparison of the supercontinuum spectra simulated in (A) Ar (6.5 bar), (B)  $N_2$  (6.5 bar), and (C)  $N_2O$  (4.4 bar) for different input pulse durations at a fixed intensity of 1 TW/cm<sup>2</sup> reveals the dynamics associated with  $\Delta n_d$ . In the molecular gases, longer pulses lead to larger degrees of molecular alignment and therefore enhanced nonlinearity. At the same time, the molecular alignment is delayed with respect to the pulse. The combination of these two effects leads to purely red-shifted supercontinuum spectra for pulse durations of approximately 100 fs in  $N_2$  and 150 fs in  $N_2O$ . Further increasing the pulse duration shifts the peak of the alignment to coincide with the trailing edge of the pulse, resulting in more symmetric spectra and optimized spectral bandwidth for pulse durations of approximately 150 fs in  $N_2$  and 280 fs in  $N_2O$ . The central frequency of the input laser was 0.29 fs<sup>-1</sup> in all cases.

coherent XUV supercontinuum spectrum through high-order harmonic generation (HHG). Last, we show that the time scale of the rotational nonlinearity can be used to shift the central frequency of the few-cycle pulses, thereby providing a more-efficient alternative to long-wavelength sources based on parametric amplification (28, 29).

### **RESULTS**

To illustrate how the dynamics of the delayed nonlinearity affect the generated supercontinuum, we calculate the spectrum generated

from propagation of laser pulses with various input pulse durations (30 fs to 1 ps) in Ar,  $N_2$ , and  $N_2O$  (Fig. 2) using a model that incorporates the delayed nonlinearities using a density matrix formalism to obtain the total nonlinear phase shift (30). While argon exhibits symmetric spectral broadening throughout, with a spectral bandwidth that quickly shrinks as the input pulse duration increases, both the molecular gases exhibit markedly different behavior depending on the input pulse duration. Both  $N_2$  and  $N_2O$  start with a broad supercontinuum at short input pulse durations, which initially shrinks with increasing pulse duration but is then followed by a

strong red shift and subsequent extension to higher frequencies. The blue-shifted components are initially weak but gradually increase in strength with further increasing input pulse duration. Notably, the supercontinuum spectra generated in  $N_2$  and  $N_2$ O with very long pulses remain substantially broader than those generated

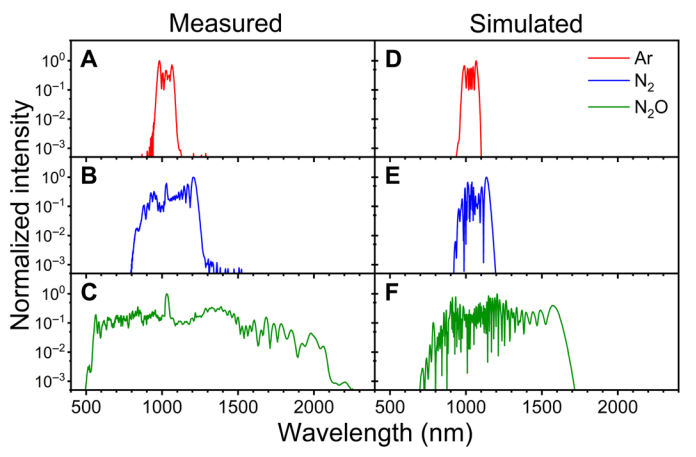


**Fig. 3. Supercontinuum spectra.** Supercontinuum spectra measured at the output of the fiber (**A** to **C**) show qualitative differences for atomic and molecular gases. Despite similar contributions from electronic Kerr nonlinearity, the spectrum from  $N_2$  is 2.4 times broader than that of Ar. Moreover, both the  $N_2$  and  $N_2$ O spectra display strong well-spaced interference modulations in the longest wavelength components, while the shortest wavelengths are comparatively smooth. This behavior is consistent with the delayed peak of the time-dependent nonlinear refractive index, which occurs on the trailing edge of the pulse as shown in Fig. 1. We additionally find qualitative agreement with spectra obtained from numerical propagation simulations (**D** to **F**) incorporating both the instantaneous and delayed response of the refractive index.

in Ar because of the enhancement afforded by the large rotational nonlinearity. For the longest pulses considered, molecular alignment approaches the adiabatic condition where  $\Delta n_d$  and  $\Delta n_i$  have the same qualitative behavior, yielding symmetric spectra with broader bandwidth than their atomic counterparts.

We experimentally demonstrate coherent supercontinuum generation by propagating 400-µJ, 280-fs pulses with a central wavelength of 1025 nm through a 3.5-m-long capillary fiber filled with Ar,  $N_2$ , or  $N_2O$ . A diagram of the experimental setup is shown in fig. S1. Pressure-dependent spectra for Ar and N<sub>2</sub> up to 6.2 bar and for N<sub>2</sub>O up to 4.4 bar are shown in fig. S2, while the spectra collected at the highest pressures are shown in Fig. 3 (A to C). The measured spectra exhibit extensions to both the short- and long-wavelength sides of the input spectrum and amplitude modulations consistent with the SPM process and with numerical propagation simulations (31) shown in Fig. 3 (D to F). In the case of  $N_2$  and  $N_2O$ , the spectral weight is shifted more heavily toward longer wavelengths, resulting in redshifted central wavelengths of 1094 and 1068 nm, respectively. This is unlike typical SPM-broadened spectra, where the generation of frequencies below and above the fundamental frequency occurs at the leading and trailing edges of the pulse, respectively, leading to a symmetric spectrum such as that observed in Ar. Instead, due to the delayed rotational nonlinearity, the zero crossing of the instantaneous frequency shift comes after the pulse's peak (Fig. 1D), leading to the enhanced generation of red-shifted frequencies.

At 6.2 bar, the supercontinuum spectra generated in Ar and  $N_2$  cover 200 and 485 nm, respectively. These correspond to bandwidth-limited pulse durations of 21 fs (six cycles at 1026 nm) and 7.4 fs (two cycles at 1094 nm) for Ar and  $N_2$ , respectively. In the case of  $N_2O$ , the supercontinuum generated at 4.4 bar covers two optical octaves and supports a bandwidth-limited pulse duration of 2.5 fs, less than one optical cycle at a central wavelength of 1068 nm. Synthesis of such short pulses requires that the phase accumulated

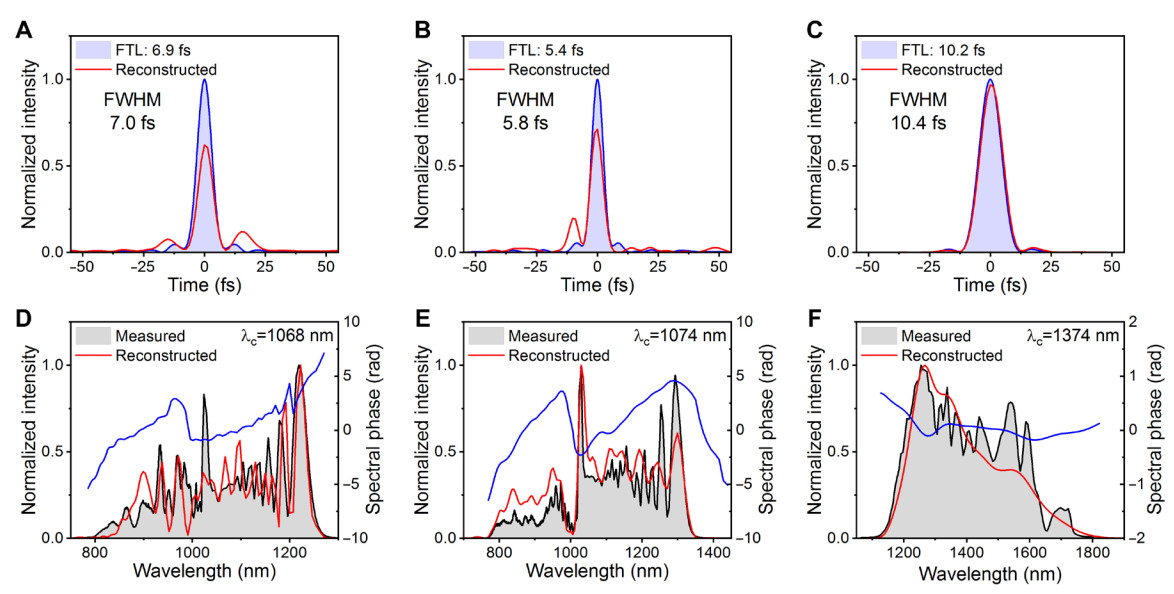


Fig. 4. Pulse compression. Retrieved temporal (A to C) and spectral intensity (D to F) profiles of few-cycle pulses obtained for the three compression demonstrations: 6.5 bar of  $N_2$  using dispersive mirrors (A and D), 2.4 bar of  $N_2$ O using dispersive mirrors (B and E), and 3.0 bar of  $N_2$ O using a programmable dispersive filter (C and F). The retrieved temporal intensity profiles (red) are normalized relative to the peak intensity of the bandwidth-limited pulse profiles (blue) calculated from the retrieved spectra. The retrieved (red) and measured (gray) spectral intensity profiles are shown along with the retrieved spectral phase (blue). In all cases, the pulses are compressed close to their bandwidth-limited durations despite the presence of residual high-order dispersion.

during propagation can be adequately compensated over the entire bandwidth. We separately demonstrate compression of the supercontinuum spectra generated in N2 and N2O to few-cycle durations in two spectral regions using dispersion-compensating mirrors (700 to 1400 nm) (32) and an acousto-optic programmable dispersive filter (1100 to 1800 nm) (33). The few-cycle pulses characterized by frequency-resolved optical gating (FROG), and their corresponding spectra, are shown in Fig. 4. Using dispersive mirrors, we generate 7.0-fs (two cycles at 1068 nm) pulses in 6.5 bar of  $N_2$  and 5.8-fs (1.6 cycles at 1074 nm) pulses in 2.4 bar of N<sub>2</sub>O, corresponding to a >45-fold compression. With the dispersive filter, we select a region of the spectrum not covered by our dispersive mirrors and demonstrate compression in the long-wavelength region of the generated supercontinuum to 10.4 fs (2.3 cycles at 1374 nm) in 3.0 bar of N<sub>2</sub>O. Last, sub-two-cycle pulses were generated in 1.0 bar of N<sub>2</sub>O using the maximum input pulse energy of 400 µJ and used to drive HHG in argon gas, where the observation of an XUV continuum reaching 80 eV (fig. S6) demonstrates the high-quality compression suitable for attosecond pulse generation. Compression efficiencies for all generated few-cycle pulses are summarized in the inset of fig. S1.

### **DISCUSSION**

The presented results underscore previously unidentified capabilities associated with the judicious choice of molecular gas media for nonlinear propagation according to the laser pulse parameters. In addition to optimizing the accumulated nonlinear phase for supercontinuum generation, we highlight a mechanism through which the laser's central frequency can be efficiently red-shifted during spectral broadening. Accordingly, for a given molecular gas, there exists a range of pulse durations that can provide either symmetric or red-shifted spectral broadening. We therefore identify propagation in molecular gases as an efficient platform for both the compression of long laser pulses, potentially yielding few-cycle pulses directly from industrial-grade picosecond lasers (34), and the generation of high-energy, longwavelength femtosecond pulses in hollow-core fibers (see the Supplementary Materials) (35). Optimistically, the use of larger linear molecules with substantially larger electronic and rotational nonlinearities and longer rotational periods (36) could potentially allow nonlinear compression of pulses with durations greater than 10 ps, which can be generated via direct amplification.

### **MATERIALS AND METHODS**

### **Experimental setup**

The experiments were performed by focusing the output of a Yb:K-GW laser amplifier (Light Conversion PHAROS: 1025 nm, 280 fs) with a maximum pulse energy and an average power of 400  $\mu$ J and 20 W, respectively, onto the entrance of a stretched hollow-core capillary fiber (few-cycle, Inc.: 3.5-m length, 500- $\mu$ m inner diameter) filled with Ar, N<sub>2</sub>, and N<sub>2</sub>O. The focal lens (f = 1 m) was mounted on a linear translation stage, allowing the distance between the lens and the fiber entrance to be varied to optimize the coupling efficiency, thereby mitigating the effects of different self-focusing lengths for the different gases. The generated supercontinuum spectra were characterized at the output of the fiber using a set of fiber-coupled spectrometers, described in more detail below. For pulse compression, spectral dispersion was compensated with either a combination of complementary-paired chirped mirrors (UltraFast Innovations PC1632)

and  $CaF_2$  glass or an acousto-optic programmable dispersive filter (AOPDF, Fastlite Dazzler UHR 900 to 1700). Temporal characterization of the few-cycle pulses was performed with a home-built second harmonic generation FROG (SHG FROG) device in single-shot geometry. HHG was performed by focusing the few-cycle pulses into an argon-filled gas cell and the emitted harmonics are dispersed with a concave flat-field grating (Hitachi 001-0640) onto a microchannel plate with phosphor screen detector.

### Spectral characterization

Because of the poor response of silicon photodetectors for wavelengths above 1 µm, we used multiple spectrometers to capture the full spectral bandwidth. For all measurements in Ar and N<sub>2</sub>, the spectra were collected using both a Si-based visible-near infrared spectrometer (Ocean Optics HR 2000 + ES) spanning 180 to 1100 nm and an indium gallium arsenide (InGaAs)-based spectrometer (Ocean Optics Flame-NIR) spanning 940 to 1660 nm. For the broader spectra generated from N2O, we used an additional cooled InGaAs-based spectrometer (Spectral Evolution IF2500) spanning 1060 to 2600 nm. Using detector response curves provided by the manufacturers, we corrected the collected spectra, interpolated the data to a common wavelength axis, and stitched them in a shared region where both spectrometers are reasonably efficient. Corrected and stitched spectra collected in Ar, N2, and N2O for various gas pressures are shown in fig. S1. Individual spectra collected using all three spectrometers for 4.4 bar of N<sub>2</sub>O, along with the detector response curves, are shown in fig. S1B to indicate how the spectra were stitched.

### **Temporal characterization**

We characterized few-cycle pulses compressed from the generated supercontinuum spectra under three different conditions. The measured and reconstructed FROG traces are shown, along with the retrieved spectra and temporal intensity profiles, in figs. S3 to S5. The specific laser parameters used in each case are also given in their respective figure captions. The FROG trace retrievals were performed using a home-built principal components generalized projections algorithm (37) on a grid of  $512 \times 512$  pixels. FROG retrieval errors are given in the captions of figs. S3 to S5. In  $N_2$  at a pressure of 6.5 bar, we obtain the best dispersion compensation when using eight bounce pairs of chirped mirrors (two reflections each on four pairs of mirrors, providing a group delay dispersion of approximately -90 fs<sup>2</sup> per pair) and 20 mm of CaF<sub>2</sub> glass (with a group velocity dispersion of approximately 19 fs<sup>2</sup>/mm at 1025 nm), resulting in pulses with a full width at half maximum (FWHM) duration of 7.0 fs (two cycles at the central wavelength of 1068 nm). In N<sub>2</sub>O at a pressure of 2.4 bar, we compress comparatively lowerenergy pulses using five bounce pairs of chirped mirrors (one reflection each on five pairs of mirrors) and 1.5 mm of CaF2, obtaining pulses with an FWHM duration of 5.8 fs (1.6 cycles at 1074 nm). We also compress a portion of the N<sub>2</sub>O spectrum not covered by our chirped mirrors (obtained using the full pulse energy at 3.0 bar) using the AOPDF, after which we obtain pulses with an FWHM duration of 10.4 fs (2.3 cycles at 1374 nm). Because of the low damage threshold of the nonlinear crystal inside the AOPDF, only a small fraction (5 µJ) of the total pulse energy was compressed using the AOPDF.

### **High-order harmonic generation**

We generate high-order harmonics by focusing the few-cycle pulses into an argon-filled cylindrical glass cell (inner diameter, 2 mm) and

characterize them using a flat-field grating spectrometer. The high harmonic spectra from the sub-two-cycle pulses were generated at a backing pressure of 90 torr, with cell centered approximately 1.7 Rayleigh lengths (3 mm) after the focus. In fig. S6, we compare the spectrum of high-order harmonics generated from a sub-two-cycle pulse compressed using N<sub>2</sub>O-filled HCF to that generated with >3-cycle pulses generated in Xe-filled HCF. As the carrier-envelope phase (CEP) of the laser was not stabilized during these measurements, the harmonic spectra are averaged over all values of CEP. For the sub-two-cycle pulse, the discrete harmonics merge into a supercontinuum spectrum. The observed harmonic cutoff of 80 eV is consistent with our estimated intensity of 200 TW/cm², based on the experimental focusing conditions, measured pulse energy, and the FROG-retrieved intensity profile.

### **SUPPLEMENTARY MATERIALS**

Supplementary material for this article is available at http://advances.sciencemag.org/cgi/content/full/6/34/eabb5375/DC1

### REFERENCES AND NOTES

- 1. F. Krausz, M. Ivanov, Attosecond physics. Rev. Mod. Phys. 81, 163-234 (2009).
- M. Chini, K. Zhao, Z. Chang, The generation, characterization and applications of broadband isolated attosecond pulses. *Nat. Photonics* 8, 178–186 (2014).
- T. Popmintchev, M.-C. Chen, D. Popmintchev, P. Arpin, S. Brown, S. Ališauskas, G. Andriukaitis, T. Balčiunas, O. D. Mücke, A. Pugzlys, A. Baltuška, B. Shim, S. E. Schrauth, A. Gaeta, C. Hernández-García, L. Plaja, A. Becker, A. Jaron-Becker, M. M. Murnane, H. C. Kapteyn, Bright coherent ultrahigh harmonics in the keV X-ray regime from mid-infrared femtosecond lasers. Science 336, 1287–1291 (2012).
- P. M. Kraus, M. Zürch, S. K. Cushing, D. M. Neumark, S. R. Leone, The ultrafast X-ray spectroscopic revolution in chemical dynamics. *Nat. Rev. Chem.* 2, 82–94 (2018).
- F. Lépine, M. Y. Ivanov, M. J. J. Vrakking, Attosecond molecular dynamics: Fact or fiction? Nat. Photonics 8, 195–204 (2014).
- 6. R. W. Boyd, Nonlinear Optics (Academic Press, ed. 3, 2008), pp. xix, 613 p.
- M. Nisoli, S. De Silvestri, O. Svelto, Generation of high energy 10 fs pulses by a new pulse compression technique. Appl. Phys. Lett. 68, 2793–2795 (1996).
- Y.-G. Jeong, R. Piccoli, D. Ferachou, V. Cardin, M. Chini, S. Hädrich, J. Limpert,
   R. Morandotti, F. Légaré, B. E. Schmidt, L. Razzari, Direct compression of 170-fs 50-cycle pulses down to 1.5 cycles with 70% transmission. Sci. Rep. 8, 11794 (2018).
- J. E. Beetar, F. Rivas, S. Gholam-Mirzaei, Y. Liu, M. Chini, Hollow-core fiber compression of a commercial Yb:KGW laser amplifier. J. Opt. Soc. Am. B 36, A33–A37 (2019).
- J. C. Travers, T. F. Grigorova, C. Brahms, F. Belli, High-energy pulse self-compression and ultraviolet generation through soliton dynamics in hollow capillary fibres. Nat. Photonics 13, 547–554 (2019).
- E. Goulielmakis, Z.-H. Loh, A. Wirth, R. Santra, N. Rohringer, V. S. Yakovlev, S. Zherebtsov, T. Pfeifer, A. M. Azzeer, M. F. Kling, S. R. Leone, F. Krausz, Real-time observation of valence electron motion. *Nature* 466, 739–743 (2010).
- A. Wirth, M. T. Hassan, I. Grguras, J. Gagnon, A. Moulet, T. T. Luu, S. Pabst, R. Santra,
   Z. A. Alahmed, A. M. Azzeer, V. S. Yakovlev, V. Pervak, F. Krausz, E. Goulielmakis,
   Synthesized light transients. Science 334, 195–200 (2011).
- M. Lenzner, C. Spielmann, E. Wintner, F. Krausz, A. J. Schmidt, Sub-20-fs, kilohertzrepetition-rate Ti:sapphire amplifier. Opt. Lett. 20, 1397–1399 (1995).
- E. Zeek, R. Bartels, M. M. Murnane, H. C. Kapteyn, S. Backus, G. Vdovin, Adaptive pulse compression for transform-limited 15-fs high-energy pulse generation. Opt. Lett. 25, 587–589 (2000).
- J. Rothhardt, S. Hädrich, A. Klenke, S. Demmler, A. Hoffmann, T. Gotschall, T. Eidam, M. Krebs, J. Limpert, A. Tünnermann, 53 W average power few-cycle fiber laser system generating soft x rays up to the water window. Opt. Lett. 39, 5224–5227 (2014).
- L. Lavenu, M. Natile, F. Guichard, X. Délen, M. Hanna, Y. Zaouter, P. Georges, High-power two-cycle ultrafast source based on hybrid nonlinear compression. *Opt. Express* 27, 1958–1967 (2019).
- S. I. Hwang, S. B. Park, J. Mun, W. Cho, C. H. Nam, K. T. Kim, Generation of a single-cycle pulse using a two-stage compressor and its temporal characterization using a tunnelling ionization method. *Sci. Rep.* 9, 1613 (2019).
- E. Haddad, R. Safaei, A. Leblanc, R. Piccoli, Y.-G. Jeong, H. Ibrahim, B. E. Schmidt,
   R. Morandotti, L. Razzari, F. Légaré, P. Lassonde, Molecular gases for pulse compression in hollow core fibers. *Opt. Express* 26, 25426–25436 (2018).
- A. Couairon, A. Mysyrowicz, Femtosecond filamentation in transparent media. *Phys. Rep.* 441, 47–189 (2007).

- O. Kwon, R. Safaei, P. Lassonde, G. Fan, A. Baltuška, B. E. Schmidt, H. Ibrahim, F. Légaré, Raman effect in the spectral broadening of ultrashort laser pulses in saturated versus unsaturated hydrocarbon molecules. Opt. Express 28, 980–990 (2020).
- S. E. Harris, A. V. Sokolov, Subfemtosecond pulse generation by molecular modulation. *Phys. Rev. Lett.* 81, 2894–2897 (1998).
- A. V. Sokolov, D. R. Walker, D. D. Yavuz, G. Y. Yin, S. E. Harris, Raman generation by phased and antiphased molecular states. *Phys. Rev. Lett.* 85, 562–565 (2000).
- A. Hoffmann, M. Zürch, M. Gräfe, C. Spielmann, Spectral broadening and compression
  of sub-millijoule laser pulses in hollow-core fibers filled with sulfur hexafluoride.

  Opt. Express 22, 12038–12045 (2014).
- A. M. Zheltikov, Understanding the nonlinear phase and frequency shift of an ultrashort light pulse induced by an inertial third-order optical nonlinearity. *Phys. Rev. A* 79, 023823 (2009).
- R. A. Bartels, T. C. Weinacht, N. Wagner, M. Baertschy, C. H. Greene, M. M. Murnane, H. C. Kapteyn, Phase modulation of ultrashort light pulses using molecular rotational wave packets. *Phys. Rev. Lett.* 88, 013903 (2001).
- N. Zhavoronkov, G. Korn, Generation of single intense short optical pulses by ultrafast molecular phase modulation. Phys. Rev. Lett. 88, 203901 (2002).
- J. K. Wahlstrand, Y.-H. Cheng, H. M. Milchberg, Absolute measurement of the transient optical nonlinearity in N<sub>2</sub>, O<sub>2</sub>, N<sub>2</sub>O, and Ar. *Phys. Rev. A* 85, 043820 (2012).
- K.-H. Hong, C.-J. Lai, J. P. Siqueira, P. Krogen, J. Moses, C.-L. Chang, G. J. Stein, L. E. Zapata, F. X. Kärtner, Multi-mJ, kHz, 2.1 μm optical parametric chirped-pulse amplifier and high-flux soft x-ray high-harmonic generation. *Opt. Lett.* 39, 3145–3148 (2014).
- F. Lu, P. Xia, Y. Matsumoto, T. Kanai, N. Ishii, J. Itatani, Generation of sub-two-cycle CEP-stable optical pulses at 35 μm from a KTA-based optical parametric amplifier with multiple-plate compression. Opt. Lett. 43, 2720–2723 (2018).
- Y. H. Chen, S. Varma, A. York, H. M. Milchberg, Single-shot, space- and time-resolved measurement of rotational wavepacket revivals in H<sub>2</sub>, D<sub>2</sub>, N<sub>2</sub>, O<sub>2</sub>, and N<sub>2</sub>O. Opt. Express 15, 11341–11357 (2007).
- X. Gao, G. Patwardhan, B. Shim, T. Popmintchev, H. C. Kapteyn, M. M. Murnane,
   A. L. Gaeta, Ionization-assisted spatiotemporal localization in gas-filled capillaries.
   Opt. Lett. 43, 3112–3115 (2018).
- R. Szipöcs, K. Ferencz, C. Spielmann, F. Krausz, Chirped multilayer coatings for broadband dispersion control in femtosecond lasers. Opt. Lett. 19, 201–203 (1994).
- P. Tournois, Acousto-optic programmable dispersive filter for adaptive compensation of group delay time dispersion in laser systems. Opt. Commun. 140, 245–249 (1997).
- C. J. Saraceno, D. Sutter, T. Metzger, M. Abdou Ahmed, The amazing progress of high-power ultrafast thin-disk lasers. J. Eur. Opt. Soc. Rapid Publ. 15, 15 (2019).
- X. Ding, M. Selim Habib, R. Amezcua-Correa, J. Moses, Near-octave intense mid-infrared by adiabatic down-conversion in hollow anti-resonant fiber. Opt. Lett. 44, 1084–1087 (2019).
- M. Reichert, H. Hu, M. R. Ferdinandus, M. Seidel, P. Zhao, T. R. Ensley, D. Peceli, J. M. Reed, D. A. Fishman, S. Webster, D. J. Hagan, E. W. Van Stryland, Temporal, spectral, and polarization dependence of the nonlinear optical response of carbon disulfide. *Optica* 1, 436–445 (2014).
- D. J. Kane, Principal components generalized projections: A review [Invited]. J. Opt. Soc. Am. B 25. A120–A132 (2008).
- C. Courtois, A. Couairon, B. Cros, J. R. Marquès, G. Matthieussent, Propagation of intense ultrashort laser pulses in a plasma filled capillary tube: Simulations and experiments. *Phys. Plasmas* 8, 3445–3456 (2001).
- M. Nurhuda, A. Suda, K. Midorikawa, M. Hatayama, K. Nagasaka, Propagation dynamics
  of femtosecond laser pulses in a hollow fiber filled with argon: Constant gas pressure
  versus differential gas pressure. J. Opt. Soc. Am. B 20, 2002–2011 (2003).
- M. Kolesik, J. V. Moloney, Nonlinear optical pulse propagation simulation: From Maxwell's to unidirectional equations. *Phys. Rev. E* 70, 036604 (2004).
- 41. T. Ditmire, T. Donnelly, A. M. Rubenchik, R. W. Falcone, M. D. Perry, Interaction of intense laser pulses with atomic clusters. *Phys. Rev. A* **53**, 3379–3402 (1996).
- F. Stutzki, C. Gaida, M. Gebhardt, F. Jansen, C. Jauregui, J. Limpert, A. Tünnermann, Tm-based fiber-laser system with more than 200 MW peak power. Opt. Lett. 40, 9–12 (2015)
- B.-H. Chen, M. Kretschmar, D. Ehberger, A. Blumenstein, P. Simon, P. Baum, T. Nagy, Compression of picosecond pulses from a thin-disk laser to 30fs at 4W average power. Opt. Express 26, 3861–3869 (2018).
- A. Baltuška, T. Udem, M. Uiberacker, M. Hentschel, E. Goulielmakis, C. Gohle, R. Holzwarth, V. S. Yakovlev, A. Scrinzi, T. W. Hänsch, F. Krausz, Attosecond control of electronic processes by intense light fields. *Nature* 421, 611–615 (2003).

**Acknowledgments:** We thank Z. Chang for loaning the infrared spectrometer and the acousto-optic programmable dispersive filter for use in the experiments. We also thank Z. Chang, E. del Barco, and E. Van Stryland for providing feedback on an earlier version of this manuscript. **Funding:** This material is based on research supported by the U.S. Department of

### SCIENCE ADVANCES | RESEARCH ARTICLE

Energy (DOE), Office of Science, Basic Energy Sciences (BES), under award no. DE-SC0019291 (M.N., T.-C.T., and M.C.) and by the Air Force Office of Scientific Research (AFOSR) under award no. FA9550-16-1-0149 (J.E.B., Y.L., and M.C.). J.N. was supported by a Summer Mentoring Fellowship from the UCF College of Graduate Studies, while O.S. and F.R. were supported by the Central Florida Physics Research Exchange Program. B.S. and G.C.N. were supported by the National Science Foundation (NSF) under award no. PHY-1707237, and the U.S. Air Force Office of Scientific Research (AFOSR) under award no. FA9550-18-1-0223. Y.W. was supported by the Air Force Office of Scientific Research (AFOSR) under award no. FA9550-15-1-0037 and by the Defense Advanced Research Projects Agency (DARPA) under award no. D18AC00011. **Author contributions:** J.E.B., M.N., and M.C. conceived and designed the study. J.E.B., M.N., T.-C.T., Y.L., J.N., and O.S. performed the experiments and analyzed experimental data under the supervision of M.C. F.R. developed the FROG reconstruction algorithm, and Y.W. provided guidance for pulse compression and characterization using the acousto-optic programmable dispersive filter. J.E.B. and M.C. performed the model calculations. G.C.N. performed the numerical simulations

under the supervision of B.S. J.E.B., M.N., B.S., and M.C. wrote the manuscript, with assistance from all authors. **Competing interests**: The authors declare that they have no competing interests. **Data and materials availability:** All data needed to evaluate the conclusions in the paper are present in the paper and/or the Supplementary Materials. Additional data related to this paper may be requested from the corresponding author.

Submitted 5 March 2020 Accepted 8 July 2020 Published 21 August 2020 10.1126/sciadv.abb5375

Citation: J. E. Beetar, M. Nrisimhamurty, T.-C. Truong, G. C. Nagar, Y. Liu, J. Nesper, O. Suarez, F. Rivas, Y. Wu, B. Shim, M. Chini, Multioctave supercontinuum generation and frequency conversion based on rotational nonlinearity. *Sci. Adv.* 6, eabb5375 (2020).

# Downloaded from https://www.science.org on January 15, 2022

# **Science** Advances

# Multioctave supercontinuum generation and frequency conversion based on rotational nonlinearity

John E. BeetarM. NrisimhamurtyTran-Chau TruongGarima C. NagarYangyang LiuJonathan NesperOmar SuarezFederico RivasYi WuBonggu ShimMichael Chini

Sci. Adv., 6 (34), eabb5375. • DOI: 10.1126/sciadv.abb5375

### View the article online

https://www.science.org/doi/10.1126/sciadv.abb5375

### **Permissions**

https://www.science.org/help/reprints-and-permissions